

MIT Open Access Articles

Speckle reduction in swept source optical coherence tomography images with slow-axis averaging

The MIT Faculty has made this article openly available. **Please share** how this access benefits you. Your story matters.

Citation: Tan, Ou, Yan Li, Yimin Wang, Martin F. Kraus, Jonathan J. Liu, Benjamin Potsaid, Bernhard Baumann, James G. Fujimoto, and David Huang. "Speckle Reduction in Swept Source Optical Coherence Tomography Images with Slow-Axis Averaging." Edited by Joseph A. Izatt, James G. Fujimoto, and Valery V. Tuchin. *Optical Coherence Tomography and Coherence Domain Optical Methods in Biomedicine XVI* (January 30, 2012). © 2012 Society of Photo-Optical Instrumentation Engineers (SPIE).

As Published: <http://dx.doi.org/10.1117/12.911735>

Publisher: SPIE

Persistent URL: <http://hdl.handle.net/1721.1/100218>

Version: Final published version: final published article, as it appeared in a journal, conference proceedings, or other formally published context

Terms of Use: Article is made available in accordance with the publisher's policy and may be subject to US copyright law. Please refer to the publisher's site for terms of use.



Speckle Reduction in Swept Source Optical Coherence Tomography Images with Slow-axis Averaging

Ou Tan^a, Yan Li^a, Yimin Wang^a, Martin F. Kraus^{b,c,d}, Jonathan J. Liu^b, Benjamin Potsaid^{b,e},
Bernhard Baumann^{b,f}, James G. Fujimoto^b, David Huang^a

^aDept. of Ophthal. and Casey Eye Inst., Oregon Health and Science Univ., Portland, OR, USA
97239

^bResearch Laboratory of Electronics and Dept. of EECS, Massachusetts Inst. of Technology,
Cambridge, MA, USA

^cSchool of Advanced Optical Technologies (SAOT), Univ. Erlangen-Nuremberg, Germany

^dPattern Recognition Lab, Univ. Erlangen-Nuremberg, Erlangen, Germany

^eAdvanced Imaging Group, Thorlabs Inc., Newton, NJ, USA 0786

^fNew England Eye Center, Tufts Univ., Boston, MA, USA

ABSTRACT

The effectiveness of speckle reduction using traditional frame averaging technique was limited in ultrahigh speed optical coherence tomography (OCT). As the motion between repeated frames was very small, the speckle pattern of the frames might be identical. This problem could be solved by averaging frames acquired at slightly different locations. The optimized scan range depended on the spot size of the laser beam, the smoothness of the boundary, and the homogeneity of the tissue. In this study we presented a method to average frames obtained within a narrow range along the slow-axis. A swept-source OCT with 100,000 Hz axial scan rate was used to scan the retina *in vivo*. A series of narrow raster scans (0-50 micron along the slow axis) were evaluated. Each scan contained 20 image frames evenly distributed in the scan range. The imaging frame rate was 417 HZ. Only frames with high correlation after rigid registration were used in averaging. The result showed that the contrast-to-noise ratio (CNR) increased with the scan range. But the best edge reservation was obtained with 15 micron scan range. Thus, for ultrahigh speed OCT systems, averaging frames from a narrow band along the slow-axis could achieve better speckle reduction than traditional frame averaging techniques.

Keywords: Swept Source Optical Coherence Tomography, Speckle Reduction, Frame Averaging, Contrast-to-noise Ratio, Slow-axis Averaging

1. INTRODUCTION

Due to its coherent imaging nature, optical coherence tomography (OCT) is prone to speckle. The speckle noise limits the signal noise ratio and degrades the image. In medical OCT images, it is difficult to distinguish small anatomical structures from the speckle noise. The speckle noise also makes the segmentation of boundaries more challenging. Therefore speckle suppression is necessary in OCT.

A number of methods have been used to reduce speckle noise in OCT, such as frame averaging[1-7] (or space compounding[8]), angular compounding,[9, 10] frequency compounding,[11] strain compounding,[12] and single B-scan filtering.[13, 14] Among them, frame averaging technique is widely used in clinical OCT systems, such as RTVue (Optovue, CA), Spectralis (Heidelberg Engineering, Heidelberg, Germany), Spectral OCT/SLO (OPKO/OTI, Miami, FL), Cirrus (Zeiss Meditec, CA) and 3D OCT-2000 (Topcon, Japan). It averages multiple frames acquired at the same location. The advantage of frame averaging is that it does not require any special designed hardware.

Recently, ultrahigh speed OCT systems with scan rate of 70K-20M Hz became available.[15-19] It takes very short time for these systems to acquire multiple frames. Frame averaging may be less efficient for speckle reduction in these systems because speckle pattern might become identical for multiple frames obtained with very high frame acquisition rate.[20] One solution is to increase time interval between two scans obtained at the same location, for example, repeating 3D volumes instead of single lines. However, when the scan speed is in the several hundred kilohertz range, special deforming registration algorithm is needed to compensate eye movements captured in 3D volumes. Such registration may take long time to perform because of its calculation complexity.

The other possible solution is to avoid the identical speckle pattern by acquiring frames within a small range along the slow-axis. The speckle patterns are less correlated as the space interval between the frames increase. On the other hand, the similarity between the images decreases when the space interval increases. Thus we should choose a proper space interval to preserve enough image similarity while the speckle patterns are least correlated between frames.

Different tissues have different boundary smoothness and texture in OCT images. For example, the retinal nerve fiber layer (NFL) has smooth boundary and does not contain high frequency texture. In contrast, the lamina cribosa and the choroid are full of high frequency textures. Therefore, the optimized space interval can be determined by pursuing smoothness in tissue with homogeneous textures and edge reservation in tissue containing high frequency textures.

In this study, we presented a method to average frames obtained within a narrow range along the slow-axis. A swept-source OCT (SS-OCT) with 100K Hz axial scan rate was used to scan the retina *in vivo*. A series of narrow raster scan ranges (0-50 micron along the slow axis), with a frame rate of 417 Hz, were evaluated by the efficiency of speckle reduction.

2. METHOD

Introduction of the swept source OCT used in this study

In this study, a SS-OCT with 100,000 Hz axial scan rate was used. The system uses a commercially available short cavity laser at 1050nm (Axsun Technologies, Billerica, MA) with 100nm tuning range. The OCT system has a measured axial resolution of 5.3 μ m (full-width-half-maximum on amplitude profile, FWHM) and imaging range of 2.9 mm in tissue. A focused spot diameter of 17.7 μ m (FWHM on amplitude profile) was calculated on the retinal plane based on the eye model in Ref[21]. In the sample arm, the average output power of the laser is 1.9 mW, consistent with safe ocular exposure limits set by the American National Standards Institute (ANSI).

Experiment

We tested a series of narrow raster scans with scan range of 0, 5, 10, 15, 20, 50 micron along the slow-axis. Each scan contained 20 evenly distributed frames. The frame rate was 417 Hz. Each scan took about 0.05 second. Each scan had 3mm scan length in the fast-axis and was obtained near the optic disc center. The scan location was chosen to acquire the lamina cribosa, nerve fiber layer, and vessel feature in the same image (Figure 1). Three scans were acquired for each scan range setting.

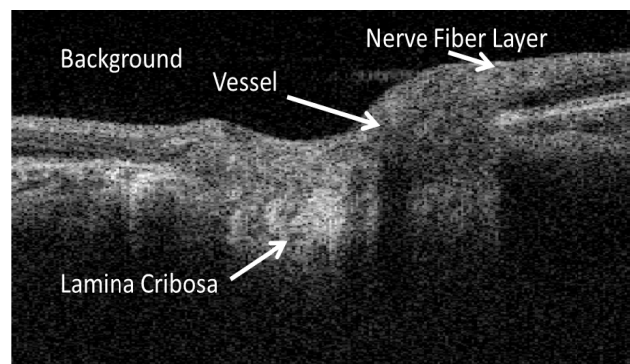


Figure 1. One single frame optical coherence tomography (OCT) image of the optical nerve head

Frame averaging

After the OCT scan was obtained, one frame was selected as the baseline frame. The other frames were aligned to the baseline frame by an automatic rigid registration along the depth and transverse (fast axis) directions. Only frames highly correlated with the baseline frame were used in averaging. The averaging is done in logarithm.

Speckle reduction evaluation

Two parameters were chosen to evaluate the speckle reduction. First, contrast-to-noise ratio (CNR) was calculated from a homogeneous and rectangle region in the NFL as signal region and the region anterior to the inner limited membrane as background[22].

$$CNR = \frac{f-b}{\sqrt{\delta_f^2 + \delta_b^2}} \quad (1)$$

Here, f is the mean intensity in signal region, b is the mean intensity in background, δ_f is the standard deviation in signal region and δ_b is the standard deviation in background.

The CNR of baseline images could be different because the scan location of the baseline frame of each scan may not be same due to eye movement and scan positioning. Thus normalized CNR was used to evaluate the image smoothing and speckle reduction. The normalized CNR was defined by the CNR of the averaged image divided by the CNR of the baseline image.

Another parameter, edge preservation index (EPI) was calculated from a rectangle region in lamina cribosa. The EPI compared the correlation between high frequency part of averaged image and baseline image[23].

$$EPI = COEF(a - \bar{a}, b - \bar{b}) \quad (2)$$

Here, COEF is the function calculating correlation coefficient of two variables, a is the intensity in lamina cribosa region of averaged image, b is the intensity in lamina cribosa region of baseline image, \bar{a} is the mean of a and \bar{b} is the mean of b . The larger EPI values indicated better preservation of image features.

3. RESULT

Visual checking of the effect of speckle reduction

The image quality of the averaged image was visually inspected for smoothness in NFL, texture pattern in lamina cribosa and contrast of vessel. Compared with single frame image (figure 1), averaged images had better image qualities for all slow-axis scan range settings. However, apparent fuzziness was observed in the averaged image with scan range=50 micron (figure 2). The smoothness of NFL increased as the scan range increased (figure 3). The texture of lamina cribosa was clear with scan range=0-15 micron (figure 4). It became slightly over-smoothed with a scan range of 20 micron. And the texture was diminished with a scan range of 50 micron (figure 4). The vessel was clear for scan range=0-15 micron. The contrast of vessels was degraded with a scan range of 20 micron. And the vessel contrast became poor with a scan range of 50 micron (figure 2).

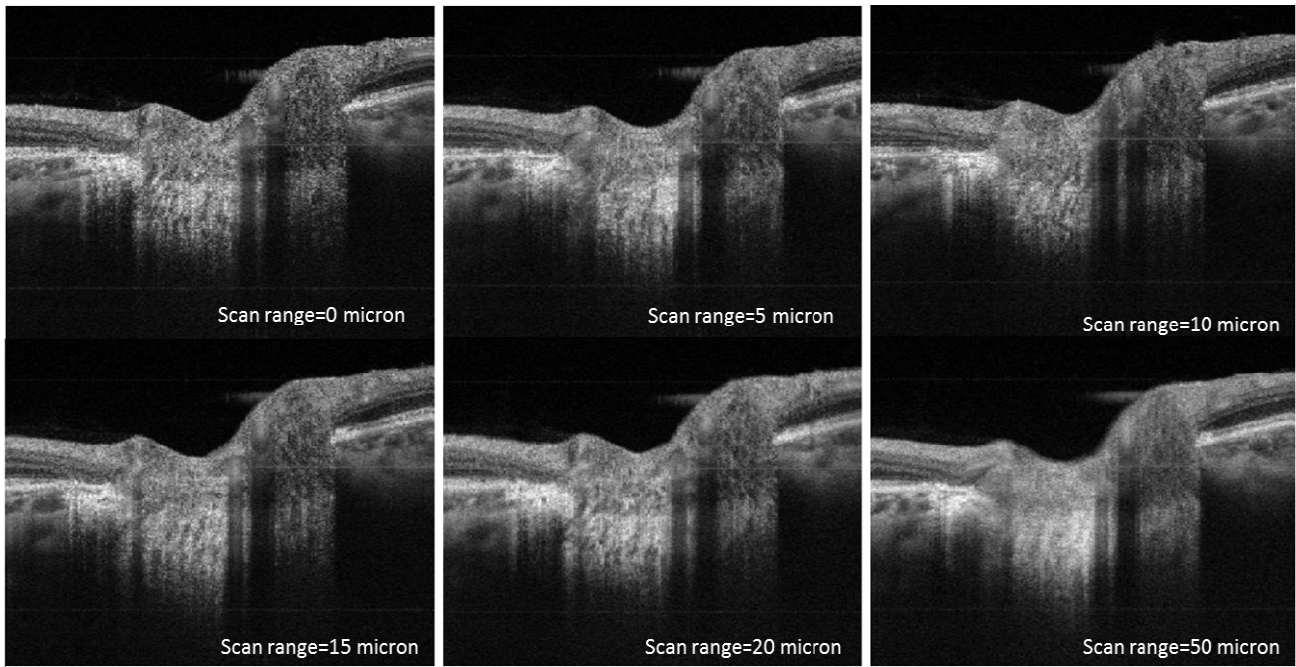


Figure 2. Averaged OCT image of the raster scan (20 frames) with different scan range along the slow-axis. Top: Left to Right, 0, 5, 10 micron scan range, respectively. Bottom, Left to Right: 15, 20, 50 microns, respectively. The single frame image is same as the one in figure 1.

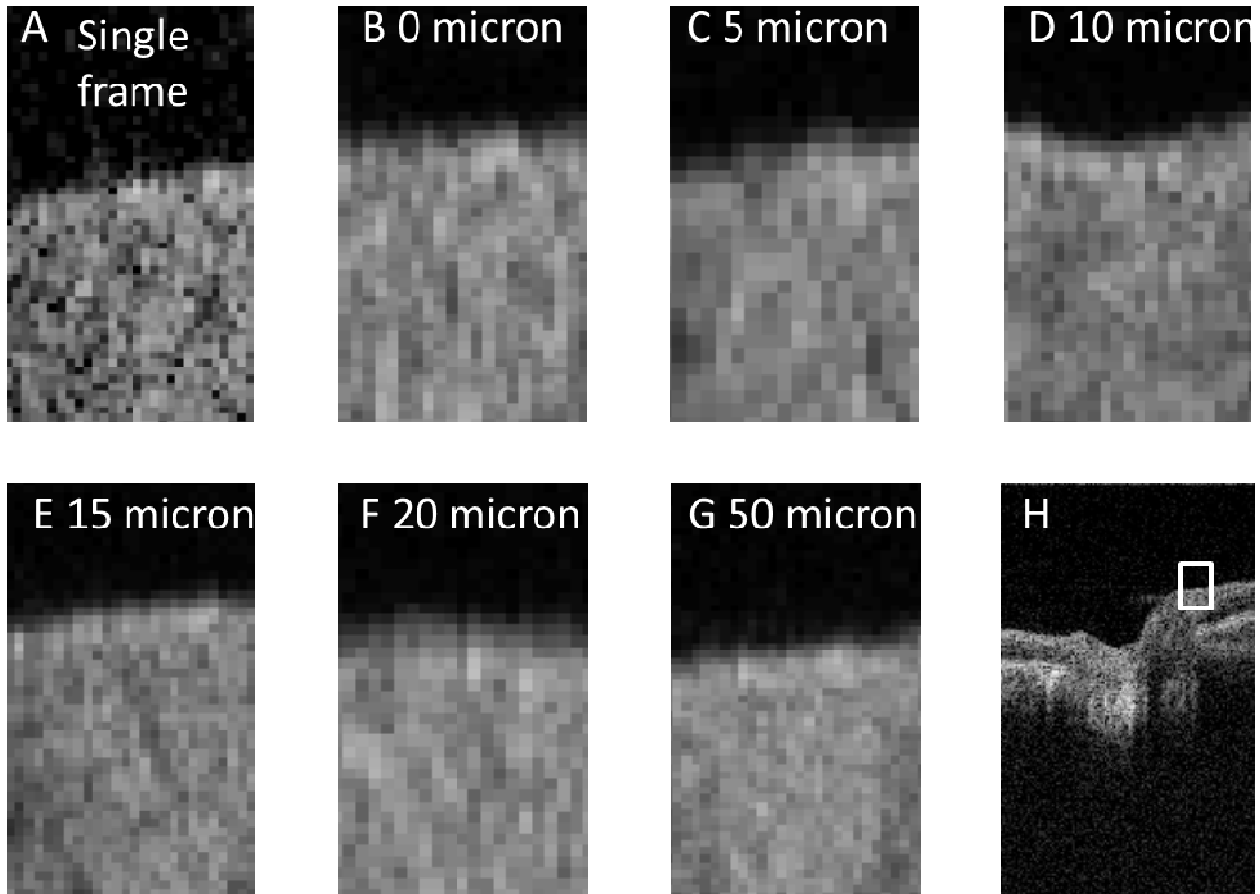


Figure 3 Enlargement (Nerve fiber layer and background) to show the smoothness after speckle reduction (A) no averaging (B)-(G) averaging of 20 frames with different scan range along the slow the slow axis, (scan range=0,5,10,15,20,50 microns). (H) The region selected in original image

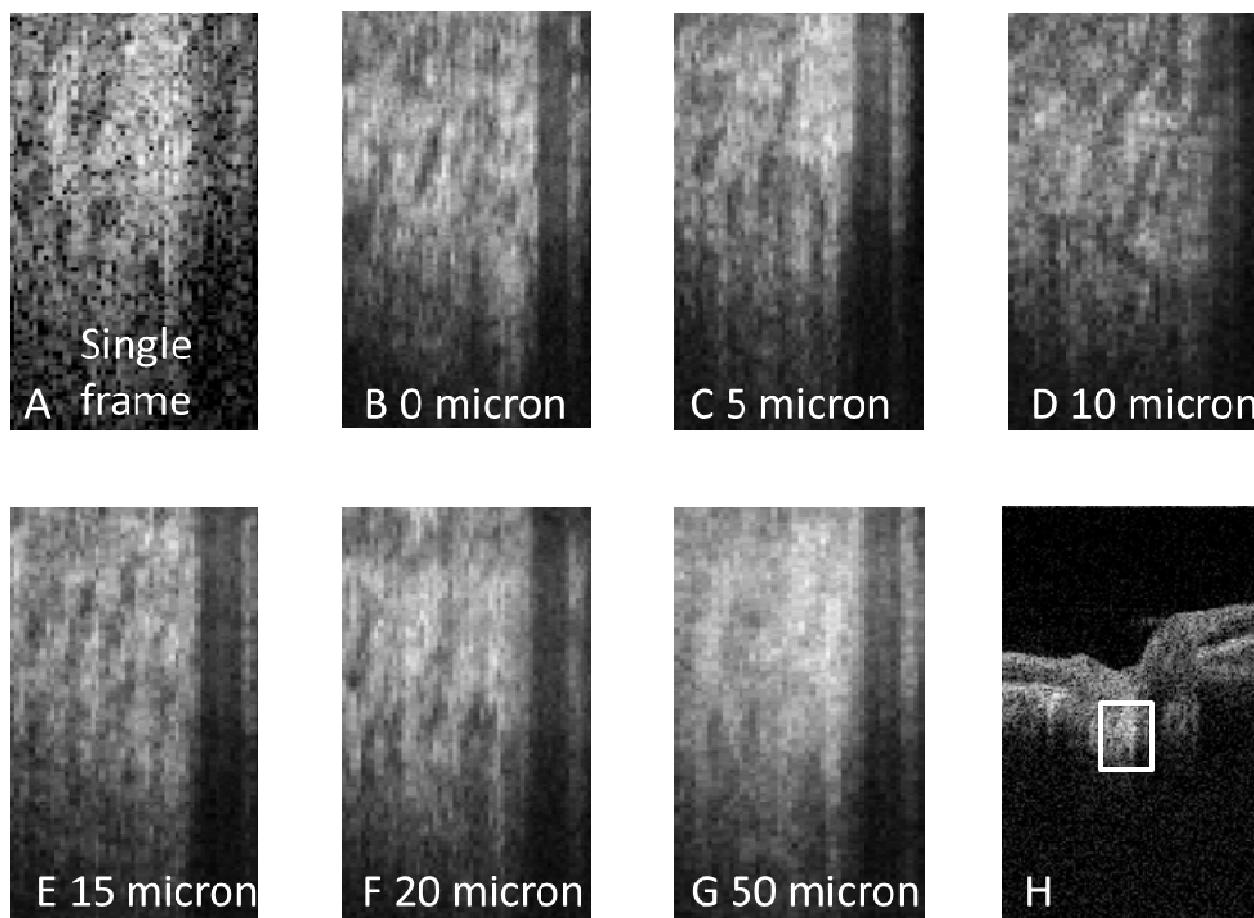


Figure 4. Enlargement (lamina cribosa) to show the smoothness after speckle reduction (A) no averaging (B)-(G) averaging of 20 frames with different scan range along the slow the slow axis, (scan range=0,5,10,15,20,50 microns). (H) The region selected in original image

Comparison of objective parameters

The values of the objective parameters agreed with the visual inspection (Table 1). A larger scan range yielded higher CNR. The EPI was similar for scan ranges between 5-15 microns and became much smaller while the scan range exceeded 20 micron. The EPI of repeated lines (scan range = 0) was also low, probably confounded by larger speckle noise or eye movement. According to our result, an optimized scan range of 15 micron along the slow-axis was recommended for the SS-OCT we used in this study.

Table 1. Normalized contrast-to- noise ratio (CNR) and edge preservation index for different scan range in slow axis direction

Slow-axis Scan Range (micron)	Normalized CNR (AVG±SD)	Edge Preservation index (AVG±SD)
0	1.60±0.07	0.31±0.04
5	1.72±0.10	0.35±0.17
10	1.71±0.07	0.36±0.11
15	1.74±0.08	0.40±0.09
20	1.92±0.12	0.28±0.04
50	2.14±0.17	0.28±0.01

Correlation between the baseline frame and other frames

In order to understand the impact of time and space intervals on the similarity of the frames, we calculated the correlation (Figure 5) between the baseline frame (10th frame) and the frames afterwards (11th-20th frames). The correlation was calculated both on low frequency and high frequency of intensity image. The correlation of low frequency represented the similarity of structure. The correlation of high frequency represented the correlation of speckle. The low frequency is calculated as the averaged intensity in a 3×3 neighborhood for each pixel. The high frequency is the original intensity subtracted by low frequency.

For scan range=0 micron, the multiple frames of a scan were obtained at the same location. It was equivalent to the traditional frame averaging method. Due to constant eye movements, such as microsaccade, small shifts in scan locations might still exist for neighboring frames obtained in this study.

The similarity of the structure decreased while the frame intervals increased (Figure 5, left). When the distance interval between neighbor frames increased, the correlation decreased faster. Specially, the 95% confidential range of similarity variation caused by eye movement (estimated using scan with a scan range=0 micron), is equal to a space interval about 15 to 20 micron (or 3-4 frames on the curve in scans with a scan range 50 micron).

The correlation of speckle decreased while the frame intervals increased (figure 5, right). For frames obtained at the same location (scan range=0 micron), the correlation of speckle was much higher if the time interval between two frames was less than 4 frames, which is equal to a time interval of 10 ms. For frame obtained at different locations, the speckle had small correlation (<0.05) when the distance between two frames exceeded 5 micron.

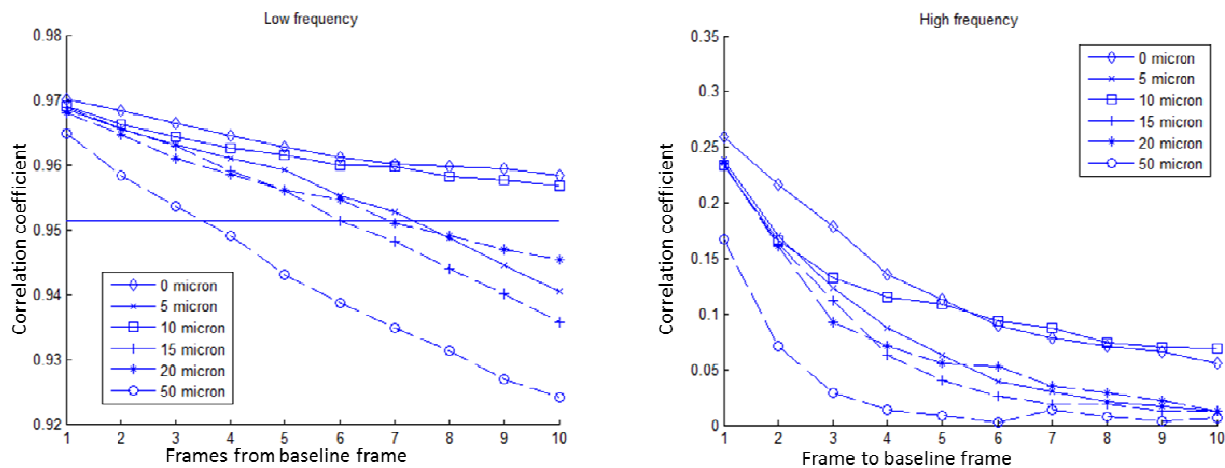


Figure 5. Correlation coefficient between baseline frame and other frames after the baseline frame. Each curve is corresponding to scan range (0-50 microns). Each point is averaged from the repeated scans in each scan setting. Notice the space interval between frames is the scan range/20; Left: Correlation coefficient of Low frequency of intensity images for scan range=0-50 micron), the horizontal line is the lower 95% confidential range of correlation coefficients for scan range=0 micron; Right: Correlation coefficient of high frequency of intensity images for scan range=0-50 micron

4. DISCUSSION

Both visual inspection and quantitative evaluation parameters revealed that speckle reduction was more effective by averaging multiple frames acquired within a narrow range along the slow-axis. Optimized smoothness and edge reservation were achieved with this technique.

The optimized scan range was close to the spot size of the laser beam. The SS-OCT system used in this study had a beam spot size of 18 micron (FWHM on amplitude profile). And its optimized slow-axis scan range was 15 micron according to the objective evaluation. If an image frame was acquired at a location more than 5 micron away from the baseline frame, the speckle correlation between them was low (Figure 5, right). However, the similarity between the two

frames was lower than the traditional frame averaging method when the space interval is larger than 15 micron (Figure 5, left). Averaging frames with low similarity will result in the loss of high frequency information. Therefore, the FWHM of the laser beam spot size gave a good estimation of the optimized scan range for retinal image.

If an image frame was acquired with more than 10 ms time interval to the baseline frame, the speckle correlation between them was low and changed slowly against the time interval (Figure 5, right). This phenomenon confirms that traditional frame averaging may work well for ophthalmologic OCT images with an imaging frame rate up to 100 Hz (i.e. 10 ms for acquiring an image frame). When the imaging frame rate exceeded the 100 Hz limitation, the traditional frame averaging might be less efficient. And one should consider averaging image frames obtained within a narrow range along the slow-axis.

This study had several limitations. The optimized value was obtained from one normal eye. A study with more subjects is needed to confirm the conclusion in this study. Moreover, the registration was only performed along depth and transverse directions with pixel-level resolution. A sub-pixel-level resolution registration may increase the correlation of registered frames, yield higher CNR, and introduce less image blurring. The scan tested in this study take 0.05 second. A shorter scan time might be needed to minimize the effect of eye movement without registration.

In summary, we provided an efficient speckle reduction method for ultrahigh speed OCT by averaging frames acquired along the slow-axis. We also designed a scheme to optimize the scan range along the slow-axis.

REFERENCES

- [1] E. Gotzinger, M. Pircher, B. Baumann *et al.*, "Speckle noise reduction in high speed polarization sensitive spectral domain optical coherence tomography," *Opt Express*, 19(15), 14568-85 (2011).
- [2] L. An, P. Li, T. T. Shen *et al.*, "High speed spectral domain optical coherence tomography for retinal imaging at 500,000 Alines per second," *Biomed Opt Express*, 2(10), 2770-83 (2011).
- [3] Z. Yuan, B. Chen, H. Ren *et al.*, "On the possibility of time-lapse ultrahigh-resolution optical coherence tomography for bladder cancer grading," *J Biomed Opt*, 14(5), 050502 (2009).
- [4] S. Bhat, I. V. Larina, K. V. Larin *et al.*, "Multiple-cardiac-cycle noise reduction in dynamic optical coherence tomography of the embryonic heart and vasculature," *Opt Lett*, 34(23), 3704-6 (2009).
- [5] Y. T. Pan, Z. L. Wu, Z. J. Yuan *et al.*, "Subcellular imaging of epithelium with time-lapse optical coherence tomography," *J Biomed Opt*, 12(5), 050504 (2007).
- [6] K. Grieve, A. Dubois, M. Simonutti *et al.*, "In vivo anterior segment imaging in the rat eye with high speed white light full-field optical coherence tomography," *Opt Express*, 13(16), 6286-95 (2005).
- [7] D. Alonso-Caneiro, S. A. Read, and M. J. Collins, "Speckle reduction in optical coherence tomography imaging by affine-motion image registration," *J Biomed Opt*, 16(11), 116027 (2011).
- [8] D. L. Marks, T. S. Ralston, and S. A. Boppart, [Data Analysis and Signal Postprocessing for Optical Coherence Tomography] Springer, 13 (2008).
- [9] N. Iftimia, B. E. Bouma, and G. J. Tearney, "Speckle reduction in optical coherence tomography by "path length encoded" angular compounding," *J Biomed Opt*, 8(2), 260-3 (2003).
- [10] Y. Watanabe, H. Hasegawa, and S. Maeno, "Angular high-speed massively parallel detection spectral-domain optical coherence tomography for speckle reduction," *J Biomed Opt*, 16(6), 060504 (2011).
- [11] M. Pircher, E. Gotzinger, R. Leitgeb *et al.*, "Speckle reduction in optical coherence tomography by frequency compounding," *J Biomed Opt*, 8(3), 565-9 (2003).
- [12] B. F. Kennedy, T. R. Hillman, A. Curatolo *et al.*, "Speckle reduction in optical coherence tomography by strain compounding," *Opt Lett*, 35(14), 2445-7 (2010).
- [13] D. C. Adler, T. H. Ko, and J. G. Fujimoto, "Speckle reduction in optical coherence tomography images by use of a spatially adaptive wavelet filter," *Opt Lett*, 29(24), 2878-80 (2004).
- [14] S. Chitchian, M. Fiddy, and N. M. Fried, "Wavelet denoising during optical coherence tomography of the prostate nerves using the complex wavelet transform," *Conf Proc IEEE Eng Med Biol Soc*, 2008, 3016-9 (2008).
- [15] M. Gora, K. Karnowski, M. Szkulmowski *et al.*, "Ultra high-speed swept source OCT imaging of the anterior segment of human eye at 200 kHz with adjustable imaging range," *Opt Express*, 17(17), 14880-94 (2009).

- [16] M. Choma, M. Sarunic, C. Yang *et al.*, "Sensitivity advantage of swept source and Fourier domain optical coherence tomography," *Opt Express*, 11(18), 2183-9 (2003).
- [17] B. Potsaid, B. Baumann, D. Huang *et al.*, "Ultra-high speed 1050nm swept source/Fourier domain OCT retinal and anterior segment imaging at 100,000 to 400,000 axial scans per second," *Opt Express*, 18(19), 20029-48 (2010).
- [18] B. Potsaid, I. Gorczynska, V. J. Srinivasan *et al.*, "Ultra-high speed spectral / Fourier domain OCT ophthalmic imaging at 70,000 to 312,500 axial scans per second," *Opt Express*, 16(19), 15149-69 (2008).
- [19] V. J. Srinivasan, D. C. Adler, Y. Chen *et al.*, "Ultra-high-speed optical coherence tomography for three-dimensional and en face imaging of the retina and optic nerve head," *Invest Ophthalmol Vis Sci*, 49(11), 5103-10 (2008).
- [20] W. Wieser, B. R. Biedermann, T. Klein *et al.*, "Multi-megahertz OCT: High quality 3D imaging at 20 million A-scans and 4.5 GVoxels per second," *Opt Express*, 18(14), 14685-704 (2010).
- [21] H. L. Liou, and N. A. Brennan, "Anatomically accurate, finite model eye for optical modeling," *J Opt Soc Am A Opt Image Sci Vis*, 14(8), 1684-95 (1997).
- [22] J. Rogowska, and M. E. Brezinski, "Evaluation of the adaptive speckle suppression filter for coronary optical coherence tomography imaging," *IEEE Trans Med Imaging*, 19(12), 1261-6 (2000).
- [23] F. Sattar, L. Floreby, G. Salomonsson *et al.*, "Image enhancement based on a nonlinear multiscale method," *Image Processing, IEEE Transactions on*, 6(6), 888-895 (1997).